Author Manuscript

Author Manuscript

Author Manuscript

Author Manuscript

HHS Public Access

Author manuscript

Ann Neurol. Author manuscript; available in PMC 2016 October 01.

Published in final edited form as:

Ann Neurol. 2015 October ; 78(4): 540–553. doi:10.1002/ana.24463.

Modulation of Creutzfeldt-Jakob disease prion propagation by the A224V mutation

Joel C. Watts, PhD[1,3,¶], **Kurt Giles, DPhil**[1,3], **Ana Serban**[1], **Smita Patel, PhD**[1], **Abby Oehler**[4], **Sumita Bhardwaj**[1], **Shenheng Guan, PhD**[1,5], **Michael Greicius, MD, MPH**[7], **Bruce L. Miller, MD**[2,3], **Stephen J. DeArmond, MD, PhD**[1,4], **Michael D. Geschwind, MD, PhD**[2,3], and **Stanley B. Prusiner, MD**[1,3,6,*]

[1]Institute for Neurodegenerative Diseases

[2]Memory and Aging Center, and Departments of

[3]Neurology

[4]Pathology

[5]Pharmaceutical Chemistry

[6]Biochemistry and Biophysics, University of California, San Francisco, San Francisco, CA 94143, USA

[7]Department of Neurology & Neurological Sciences, Stanford University, Stanford, CA 94305, USA

Abstract

Objective—Mutations in the gene encoding the prion protein (PrP) are responsible for approximately 10–15% of cases of prion disease in humans, including Creutzfeldt-Jakob disease (CJD). Here we report the discovery of a previously unreported C-terminal PrP mutation (A224V) in a CJD patient exhibiting a disease similar to the rare VV1 subtype of sporadic CJD and investigate the role of this mutation in prion replication and transmission.

Methods—We generated transgenic (Tg) mice expressing human PrP with the V129 polymorphism and A224V mutation, denoted Tg(HuPrP,V129,A224V) mice, and inoculated them with different subtypes of sporadic (s) CJD prions.

Results—Transmission of sCJD VV2 or MV2 prions was accelerated in Tg(HuPrP,V129,A224V) mice compared to Tg(HuPrP,V129) mice, with incubation periods of ~110 days and ~210 days, respectively. In contrast, sCJD MM1 prions resulted in longer

*To whom correspondence should be addressed at: 675 Nelson Rising Ln, Room 318, San Francisco, CA 94143-0518; Tel: (415) 476-4482; Fax: (415) 476-8386; stanley@ind.ucsf.edu.

¶Present address: Tanz Centre for Research in Neurodegenerative Diseases, University of Toronto, Toronto, Ontario, Canada, M5T 2S8

Authorship

J.C.W., K.G., B.M., M.D.G., and S.B.P. contributed to conception and design of the study; J.C.W., K.G., A.S., S.P., A.O., S.B., S.G., M.G., S.J.D., and M.D.G. contributed to data collection and analysis; and J.C.W., K.G., M.D.G., and S.B.P. contributed to writing the manuscript.

Potential conflicts of interest

The Institute for Neurodegenerative Diseases has a research collaboration with Daiichi Sankyo (Tokyo, Japan).

Author Manuscript Author Manuscript Author Manuscript Author Manuscript

incubation periods in Tg(HuPrP,V129,A224V) mice compared to Tg(HuPrP,V129) mice (~320 days v. ~210 days). Prion strain fidelity was maintained in Tg(HuPrP,V129,A224V) mice inoculated with sCJD VV2 or MM1 prions, despite the altered replication kinetics.

Interpretation—Our results suggest that A224V is a risk factor for prion disease and modulates the transmission behavior of CJD prions in a strain-specific manner, arguing that residues near the C-terminus of PrP are important for controlling the kinetics of prion replication.

INTRODUCTION

The prion diseases caused by the prion protein (PrP) are a group of orphan disorders caused by invariably fatal neurodegeneration in both humans and animals [1]. In humans, approximately 85% of all PrP prion disease cases are sporadic with the majority being classified as sporadic (s) Creutzfeldt-Jakob disease (CJD). Heritable forms of these disorders, such as familial (f) CJD, Gerstmann-Sträussler-Scheinker disease (GSS), and fatal familial insomnia (FFI) account for approximately 10–15% of cases and are caused by mutations in the *PRNP* gene, which encodes PrP. Human prion diseases that are acquired via an infectious route comprise <1% of cases and include variant (v) CJD.

In the PrP prion diseases, the cellular isoform of PrP (PrP^{C}), which is predominantly α-helical, adopts an alternative conformation that becomes self-propagating. In contrast to PrP^{C}, the pathogenic isoform PrP^{Sc} is enriched in β-sheets and exhibits propensity to assemble into oligomers as well as amyloid fibrils. During replication, PrP^{Sc} templates the conformational conversion of PrP^{C} into nascent copies of PrP^{Sc}; this self-propagating process enables the multiplication and spread of prions throughout the brain and ultimately results in spongiform (vacuolar) degeneration, PrP^{Sc} deposition, astrocytic gliosis, and neuronal dysfunction. PrP^{Sc} can be differentiated from PrP^{C} by digestion with proteases such as proteinase K (PK): whereas PrP^{C} is completely sensitive to PK digestion, PrP^{Sc} is partially resistant [2]. Digestion of human PrP^{Sc} with PK and PNGase F typically results in a PK-resistant core with a molecular mass of either ~21 kDa or ~19 kDa, which are referred to as “Type-1” or “Type-2” PrP^{Sc}, respectively [3]. Type-1 and Type-2 PrP^{Sc} constitute distinct strains of prions, which are thought to represent different structures of PrP^{Sc} [4, 5].

A common polymorphism exists in human (Hu) PrP at codon 129, where either a methionine (M) or valine (V) residue can be present. Sporadic CJD can be classified into distinct disease subtypes according to the patient’s codon-129 genotype (MM, MV, or VV) and the presence of Type-1 or Type-2 PrP^{Sc} in the brain [3, 6]. The most common subtypes are MM1, VV2, and MV2, whereas VV1 accounts for only ~1–2% of all sCJD cases [3, 7]. CJD prions can be transmitted to transgenic (Tg) mice expressing human HuPrP, and transmission is most efficient when the recipient Tg mice express an allele that matches the PrP^{Sc} sequence in the CJD patient. For example, sCJD VV2 prions transmit disease efficiently to Tg mice expressing HuPrP(V129) in ~200 days but do not infect Tg mice expressing HuPrP(M129) [8, 9].

Here, we identify a novel C-terminal PrP mutation (A224V) in a CJD patient homozygous for valine at codon 129 and with Type-1 PrP^{Sc} in the brain. Tg mice expressing HuPrP(V129) with the A224V mutation exhibited shorter incubation periods upon

Author Manuscript Author Manuscript Author Manuscript Author Manuscript

inoculation with sCJD VV2 or MV2 prions compared to Tg(HuPrP,V129) mice, without any apparent alteration in prion strain properties. Our findings argue that the kinetics of prion replication can be modulated by residues near the C-terminus of PrP and suggest that A224V is a prion disease risk factor.

MATERIALS AND METHODS

Evaluation of the CJD(A224V) patient

Clinical brain MRI with diffusion weight imaging (DWI) was performed on a 1.5T magnet with sedation. Levels of neuron-specific enolase in the CSF were determined at the Mayo Laboratory and levels of total tau in the CSF were determined by Athena Diagnostics. Sequencing of the *PRNP* gene was performed at the National Prion Disease Pathology Surveillance Center.

Generation of transgenic mice

Tg mice expressing wt or mutant A224V HuPrP(V129) under the control of the Syrian hamster *Prnp* promoter were generated as described previously [10] and were maintained by backcrossing to FVB-*Prnp*$^{0/0}$ mice [11]. Transgene expression levels relative to the level of PrP expression in wt FVB mice were determined by sandwich ELISA [12] using F20-108a [13] as the capture antibody and HRP-labeled HuM-P [14] as the detection antibody.

Mouse lines

All mice were maintained on an FVB-*Prnp*$^{0/0}$ background, and all Tg lines were maintained in a hemizygous state, except Tg152 mice [15] and Tg2669 mice [10], both of which were maintained in a homozygous state. Bigenic Tg8422/152 and Tg8422/2669 lines were created by crossing hemizygous Tg8422 mice with homozygous Tg152 or homozygous Tg2669 mice, respectively.

Prion bioassays

Brain samples for prion bioassays were obtained from pathologically confirmed and genotyped cases of sCJD exhibiting the VV1, VV2, MV2, or MM1 disease subtypes as well as the brainstem of the CJD(A224V) patient. Frozen brain material was thawed and then homogenized to 10% (wt/vol) using a bead beater (PreCellys) and then further diluted to 1% (wt/vol) in 5% BSA prior to inoculation into mice. Prion inoculations and disease monitoring were conducted as described previously [16]. The Log-rank (Mantel-Cox) test was used to assess statistical differences in the survival curves between different groups of inoculated mice using Prism 5 software (GraphPad Software). All animal experiments were performed under biosafety level 3 (BSL-3) containment conditions using protocols approved by the Institutional Animal Care and Use Committee (IACUC) at the University of California San Francisco (UCSF). UCSF is accredited by the Association for Assessment and Accreditation of Laboratory Animal Care (AAALAC).

Author Manuscript Author Manuscript Author Manuscript Author Manuscript

Immunoblotting and protease digestions

Frozen mouse or human brain samples were thawed and then homogenized to final concentration of 10% (wt/vol) in PBS lacking calcium and magnesium (Life Technologies) using a bead beater homogenizer (PreCellys). PK digestion reactions using a final PK concentration of 50 μg/mL as well as immunoblotting experiments were performed as previously described [16] using the anti-PrP antibody HuM-P at a concentration of 0.1–0.2 μg/mL.

Conformational stability assays

Conformational stability assays for PrP^{Sc} upon exposure to increasing concentrations of guanidine hydrochloride (GdnHCl) were conducted as described previously [16].

Neuropathology

A brain-only autopsy of the CJD(A224V) patient was performed at UCSF. Sections were fixed in 10% buffered formalin, embedded in paraffin, and 8-μm-thick slices cut. The sections were stained with hematoxylin and eosin (H&E) to evaluate the degree and type of vacuolation; by immunohistochemistry using the anti-PrP monoclonal antibody 3F4 (with hydrolytic autoclaving to eliminate PrP^{C} staining); by GFAP immunohistochemistry to determine the degree and distribution of reactive astrocytic gliosis; by the Bielschowsky silver stain for axons; and the Nissl stain to estimate the degree of nerve cell body loss. For neuropathological analysis of mouse brains, mice were euthanized and then brains were removed, fixed in 10% buffered formalin, and then embedded in paraffin. H&E staining as well as immunohistochemistry for PrP^{Sc} using the antibody 3F4 was performed as previously described [16].

Characterization of wt and mutant PrP^{Sc} by mass spectrometry

PrP^{Sc} was purified from the frontal lobe of the CJD(A224V) patient using PK digestion and phosphotungstic acid precipitation, and then the GPI anchor and N-linked oligosaccharides were removed by digestion with PIPLC and PNGaseF, respectively. Proteins were reduced, alkylated, and then fractionated by SDS-PAGE. Based on the migration of molecular weight markers, regions predicted to contain PrP^{Sc} were excised from the gel and then trypsinized. Tryptic peptides were analyzed by LC-MS/MS on an LTQ Orbitrap XL mass spectrometer equipped with a NanoAcquity LC system. Standard curves of peptide concentrations against extracted ion chromatogram peak areas were generated using synthetic peptides ESQAYYQR and ESQVYYQR, and were used to calculate the concentrations of wt (A224) and mutant (V224) PrP^{Sc} peptides in the brain of the CJD(A224V) patient. Statistical differences were assessed using a paired two-sided *t*-test test with a significance threshold of $P = 0.05$.

RESULTS

Clinical evaluation of the CJD(A224V) patient

A 49-year-old woman was referred to our center with suspected CJD. The onset of symptoms occurred 10 months earlier, when her colleagues first noted brief memory lapses.

Author Manuscript Author Manuscript Author Manuscript Author Manuscript

By 6 months post-onset, she developed problems with planning and organization. By month 8 post-onset, she stopped driving because she no longer remembered how to get to even local, familiar places. At 9 months following the onset of symptoms, she was evaluated at a memory clinic, in which an antibody-mediated paraneoplastic syndrome was suspected, but the brain MRI was noted to be suggestive for CJD. Between months 9–10 post-onset, she became more confused, was getting lost at home, developed mild irritability, began walking slower, developed a right hand tremor, and began needing reminders to shower. A comprehensive metabolic, infectious, cancer, and autoimmune/paraneoplastic screen was unrevealing.

Ten months after the onset of symptoms, she was seen at UCSF for a second opinion regarding a diagnosis of CJD. Cognitively, she had significant problems with short-term memory, was extremely perseverative, and was not oriented to the month, year, or her age. CSF showed normal protein (39 mg/dl) and glucose (86 mg/dl), but elevated levels of neuron-specific enolase (39 ng/ml) and total tau (6,300 pg/ml), both of which are consistent with CJD [17, 18]. Electroencephalograms (EEG) did not reveal any periodic sharp wave complexes (PSWC). A repeat MRI conducted 3 weeks after the initial MRI revealed cortical ribboning and striatal hyperintensities on DWI, with restricted diffusion, which was consistent with CJD [19, 20] (Fig. 1A).

Genetic testing revealed a heterozygous C-to-T transition mutation at position 671 of the *PRNP* open reading frame, which resulted in a novel alanine to valine substitution at codon 224 of HuPrP. The patient was homozygous for valine at polymorphic codon 129, indicating that the A224V mutation was in *cis* to V129. The patient had no family history of dementia or neurodegenerative disease. Her mother died from confirmed brain cancer in her 70s. Her father was alive and healthy in his late 70s and carried the A224V mutation but with heterozygosity (MV) at codon 129. She was treated with quinacrine and doxycycline on a compassionate basis for CJD, but continued to progress. She stopped walking and became bedbound over the next several months, requiring extensive 24-hour nursing care. She died in a vegetative state 32 months after onset.

Pathological and biochemical evaluation of the CJD(A224V) patient's brain

Severe, bilateral cortical atrophy was observed in the frontal lobes of the CJD(A224V) patient's brain, and moderately severe atrophy was found in the parietal, temporal, and occipital lobes. The main histopathological features were severe degeneration and loss of neurons. Because of the severe loss of neurons, the typical intraneuronal spongiform degeneration of CJD was replaced in most cortical regions with a large, irregular, and extracellular pattern of vacuolation designated status spongiosis (Fig. 1B). Immunohistochemistry for PrP revealed densely packed, finely granular PrP^{Sc} deposits, which were most intense in layers 2–6 and less intense in layer 1 (Fig. 1C), confirming the diagnosis of CJD. A very intense reactive astrocytic gliosis filled the entire cerebral cortex (Fig. 1D), underlying white matter, and striatum. Nissl staining revealed 60–80% loss of cortical neurons in the prefrontal lobe (Fig. 1E), parietal lobe, medial occipital lobe, and insula. The cerebellar cortex contained vacuoles in the molecular layer, marked loss of Purkinje cells, and greater than 50% loss of granule cell neurons (Fig. 1F). PrP^{Sc} deposits

Author Manuscript Author Manuscript Author Manuscript Author Manuscript

were found throughout the cerebellar cortex (Fig. 1G) and were associated with intense reactive Bergman radial glia in the molecular layer and intense reactive astrocytic gliosis in the Purkinje and granule cell layers (Fig. 1H). Loss of neurons from the dentate nucleus was 30–50% and was reflected in the development of proximal Purkinje cell axonal swellings (torpedoes) (arrows in Fig. 1F, H, and I). No neurofibrillary tangles were observed.

The brain of the CJD(A224V) patient contained abundant PK-resistant PrP (Fig. 1J). The unglycosylated PK-resistant PrP band migrated to ~21 kDa following electrophoresis (Fig. 1K), consistent with Type-1 PrP^{Sc}. To determine the relative levels of mutant and wt PrP^{Sc} in the CJD(A224V) patient, we partially purified protease-resistant PrP^{Sc} from the patient's brain and then performed mass spectrometry. Wild-type (A224) and mutant (V224) PrP^{Sc} were found in roughly equal proportions in the CJD(A224V) patient's brain (Fig. 1L).

Transmission of CJD(A224V) prions to transgenic mice

We next performed transmission studies with the CJD(A224V) prions in Tg(HuPrP,V129)152 mice, denoted Tg152, which express wt HuPrP(V129). For comparison, we also transmitted a sample from an sCJD patient exhibiting the VV1 disease subtype. Both the CJD(A224V) and sCJD VV1 cases transmitted disease with 100% efficiency to Tg152 mice (Table 1, Fig. 2A). The brains of CJD(A224V)- and sCJD VV1-inoculated Tg152 mice contained Type-1 PrP^{Sc} species similar to the inoculum (Fig. 2B), suggesting that the properties of the prion isolates remained unchanged. Intense spongiform degeneration was observed in the cerebral cortex and striatum of mice inoculated with CJD(A224V) (Fig. 2C, D), and large numbers of granular PrP^{Sc} deposits, similar to those observed in the CJD(A224V) patient's brain, were evident in the granule cell layer of the cerebellum and the thalamus (Fig. 2E, F). Similar neuropathological changes were apparent in the sCJD VV1-inoculated animals (Fig. 2G–J). No obvious differences in the distribution of vacuolation or PrP^{Sc} deposition patterns were observed between CJD(A224V)- and sCJD VV1-inoculated Tg152 mice.

Generation of Tg(HuPrP,V129,A224V) mice and transmission studies

To investigate the role of the A224V mutation in the formation and replication of prions, we generated Tg mice expressing HuPrP(V129) with the A224V substitution. Four lines of mice were obtained, with levels of PrP expression ranging from 1.5- to 3.2-fold the levels observed in the brains of non-Tg mice (Fig. 3A, Table 1). We also generated three additional lines of mice expressing wt HuPrP(V129), with 2.6- to 4.5-fold levels of PrP expression in the brain. Tg lines expressing wt HuPrP(V129) or mutant HuPrP(V129,A224V) were observed for ~600 days, and none developed any signs of spontaneous neurologic illness (Table 1) nor exhibited any PK-resistant PrP (Fig. 3B) or prion disease-specific neuropathological changes in their brains (not shown). Clinical disease was not observed in Tg(HuPrP,V129,A224V) mice inoculated with CJD(A224V) prions during an observation period of greater than 500 days (Table 1). However, 5 of 5 CJD(A224V)-challenged Tg18807 mice examined at 543 days postinoculation exhibited abundant Type-1 PK-resistant PrP^{Sc} in their brains (Fig. 3C). Similarly, sCJD VV1 prions transmitted disease to a subset of Tg8422 mice with an incubation period of ~540 days (Table 1, Fig. 3C),

Author Manuscript Author Manuscript Author Manuscript Author Manuscript

suggesting that the VV1 subtype of CJD prions propagates more slowly in mice expressing mutant PrP(A224V) than in mice expressing wt PrP.

To determine if the A224V mutation can modulate the transmission of other CJD prions, we challenged the eight lines of Tg(HuPrP,V129) and Tg(HuPrP,V129,A224V) mice with two different sCJD isolates: VV2 “case i” and an MM1 case (Table 1). Whereas prions from sCJD VV2 case i transmitted disease to Tg(HuPrP,V129) mice with mean incubation periods of ~200 days, Tg(HuPrP,V129,A224V) mice inoculated with the same isolate required approximately half the time (105–128 days) to develop disease (Table 1, Fig. 4A). The brains of clinically ill Tg mice injected with VV2 case i harbored Type-2 PK-resistant PrP^{Sc}, as was observed for the inoculum (Fig. 4B). In contrast, the mean incubation periods for MM1 prions in Tg(HuPrP,V129,A224V) mice (224–325 days) were longer than those observed in the Tg(HuPrP,V129) mice (206–233 days) (Table 1, Fig. 4C). Tg mice injected with MM1 prions contained Type-1 PK-resistant PrP^{Sc}, similar to the inoculum (Fig. 4B). Among the Tg(HuPrP,V129,A224V) lines, the PrP expression levels and incubation periods were inversely correlated for VV2 prions and directly correlated for MM1 prions (Fig. 4D). To determine the reproducibility of our findings, we bioassayed additional sCJD samples in Tg152 and Tg8422 mice (Table 2). A second sCJD VV2 isolate (“case ii”) as well as an sCJD MV2 case both transmitted disease with significantly shorter incubation periods in Tg8422 mice than Tg152 mice ($P < 0.001$, Fig. 4A, Table 2). The brains of clinically ill Tg152 or Tg8422 mice inoculated with sCJD VV2 case ii or MV2 prions contained Type-2 PK-resistant PrP^{Sc} (Fig. 4E).

To determine whether the relatively shorter incubation periods for VV2 prions and longer incubation periods for MM1 prions were due to transmission barrier effects, we performed second passage experiments in Tg(HuPrP,V129,A224V) mice. The incubation period for sCJD VV2 prions was unchanged upon second passage in either the Tg8422 or Tg18807 lines (Table 1), and the incubation period for sCJD MM1 prions in Tg18807 mice upon second passage was slightly extended compared to the first passage (252 v. 224 days). Thus, transmission barriers were unlikely to feature during passage of VV2 or MM1 prions in Tg(HuPrP,V129,A224V) mice.

The brains of sCJD VV2-inoculated Tg152 mice contained plaque-like PrP^{Sc} deposits in the corpus callosum (Fig. 5A). Similar deposits were found in the brains of Tg8422 mice following one or two passages of sCJD VV2 prions (Fig. 5B, C), arguing for the maintenance of strain fidelity. We also performed conformational stability assays, which are commonly used to distinguish different strains of prions, on PK-resistant PrP^{Sc} in the brains of sCJD VV2-inoculated Tg152 and Tg8422 mice. The denaturation profiles (Fig. 5D) and denaturation curves (Fig. 5E) were similar for sCJD VV2 prions propagated in either Tg152 or Tg8422 mice and yielded $[GdnHCl]_{1/2}$ values that were not significantly different from each other (1.65 ± 0.05 M and 1.70 ± 0.09 M, respectively).

As a final test of strain fidelity, we performed a “retrotransmission” experiment in which sCJD VV2 prions that had been propagated in Tg(HuPrP,V129,A224V)18807 mice were reinoculated into Tg152 mice expressing wt HuPrP(V129). The survival curves for Tg152 mice inoculated with sCJD VV2 prions or with sCJD VV2 prions passaged once in Tg18807

Author Manuscript Author Manuscript Author Manuscript Author Manuscript

mice were not significantly different from each other (Fig. 5F). Moreover, the Type-2 PrP^{Sc} of the sCJD VV2 strain was maintained upon retrotransmission, and the banding patterns of PrP^{Sc} from the original sCJD VV2 inoculum, passaged sCJD VV2, and retrotransmitted sCJD VV2 prions were indistinguishable (Fig. 5G). Cumulatively, these results indicate that the fidelity of the sCJD VV2 strain was maintained upon passage in Tg(HuPrP,V129,A224V) mice, despite their rapid incubation periods.

We were curious whether the simultaneous presence of wt HuPrP alleles may influence the ability of mutant HuPrP(V129,A224V) to accelerate the replication of sCJD VV2 prions. Therefore, we generated bigenic mice coexpressing mutant HuPrP(V129,A224V) and either wt HuPrP(V129) or HuPrP(M129), denoted as Tg8422/152 and Tg8422/2669 mice, respectively. Tg152 and Tg2669 mice express similar levels of HuPrP in their brains [10, 15]. A proportion of Tg8422/152 and Tg8422/2669 mice exhibited ataxia and circling behavior beginning at ~500 days of age (Table 2). However, neither insoluble, PK-resistant PrP (Fig. 6A) nor prion disease-specific neuropathological changes (not shown) were found in the brains of these animals, arguing that the spontaneous signs of neurologic illness derive from prolonged overexpression of PrP [21].

The incubation period for sCJD VV2 case i in bigenic Tg8422/152 mice was slightly longer (~130 days) compared to Tg8422 mice (~110 days; Table 2), arguing that coexpressing wt HuPrP(V129) has only a minimal, if any, effect on the ability of HuPrP(V129,A224V) to propagate sCJD VV2 prions. In contrast, the incubation period for sCJD VV2 in Tg8422/2669 mice was ~200 days (Fig. 6B), implying that wt HuPrP(M129) interfered with the ability of HuPrP(V129,A224V) to propagate sCJD VV2 prions. Because the PK-resistant PrP^{Sc} isoforms were similar in the brains of sCJD VV2-infected Tg8422/152 and Tg8422/2669 mice (Fig. 6C), this finding argued that the presence of HuPrP(M129) did not alter the properties of the sCJD VV2 prions. Because sCJD VV2 prions did not transmit robustly to mice expressing HuPrP(M129) [8, 22], we speculate that the presence of HuPrP(M129) in *trans* abrogates the enhanced kinetics of sCJD VV2 prion replication in Tg(HuPrP,V129,A224V) mice.

DISCUSSION

In the studies described here, we demonstrate that a previously unreported C-terminal PrP mutation found in a patient with CJD is capable of modulating the replication kinetics of four distinct strains of CJD prions (MM1, VV2, MV2, and VV1). An important issue is whether the A224V mutation causes disease or is a rare polymorphism that was found by coincidence in an sCJD patient exhibiting the VV1 subtype. Indeed, several *PRNP* mutations that were originally believed to be pathogenic are now thought to instead constitute uncommon polymorphisms, as they have been found in patients without any family history of prion disease, including long-lived asymptomatic individuals who carry the "mutation" and those whose autopsies show no evidence of prion disease [23, 24]. Definitive proof of the disease-causing nature of the A224V mutation will require the emergence of additional cases. However, our finding that A224V modifies the kinetics of prion replication strongly suggests that the mutation is a risk factor for prion disease.

Author Manuscript Author Manuscript Author Manuscript Author Manuscript

A survey of ~3600 control and prion disease patients did not identify any individuals with the A224V substitution [24]. Moreover, sequencing data from the Exome Aggregation Consortium (ExAC) reveal that the A224V mutation was not found in more than 60,000 individuals without a neurodegenerative disease phenotype [25], suggesting that A224V is unlikely to be a rare, benign polymorphic variant. Because VV1 is the rarest subtype of sCJD, accounting for only ~1–2% of all sCJD cases [3, 7] and thus occurring at a frequency of 1–2 cases per 100 million people, it is unlikely that a previously unobserved polymorphism would be first discovered by chance in a patient with sCJD VV1.

The strongest evidence against the causative nature of the A224V mutation is that the patient's father also possesses the mutation but remains asymptomatic, potentially suggesting that the mutation alone is inadequate to confer a disease phenotype. Several explanations seem plausible. The A224V mutation may have incomplete penetrance, as has been suggested for the V210I mutation [26], or may exhibit a highly variable age of disease onset, as has been observed with the E200K mutation [27]. The patient's father could also exhibit somatic mosaicism for the mutation, resulting in the mutant allele only being expressed in a minority of cells in the brain [28]. Alternatively, the gene product of the non-mutant PrP allele may play a crucial role. The CJD(A224V) patient was VV homozygous at polymorphic codon 129, whereas the patient's father is MV heterozygous at this locus. Sporadic CJD is known to occur more frequently in patients who are homozygous at codon 129 [29], and the disease course has been reported to be prolonged in FFI patients who are heterozygous at codon 129 [30]. We found that the PK-resistant PrP in the CJD(A224V) patient's brain was composed of both wt and mutant A224V PrP^{Sc}, suggesting that the wt and mutant PrP alleles interact with each other. Indeed, we discovered that the ability of the A224V mutation to accelerate the kinetics of sCJD VV2 prion replication was abrogated with the coexpression of wt HuPrP(M129), but not with wt HuPrP(V129). Thus, the presence of wt HuPrP(M129) in the patient's father may prevent or impede the formation of prions specified by the A224V mutation.

Based on the transmission properties of the CJD(A224V) and sCJD VV1 isolates, we were unable to identify differences in the prion strains. However, this does not preclude a causative role for the A224V mutation since fCJD caused by the E200K mutation and sCJD MM1 are clinically and pathologically indistinguishable and exhibit identical transmission properties in Tg mice and bank voles [15, 31, 32]. There were some clinical and pathological overlaps of our CJD(A224V) patient with sCJD VV1 cases, in that both have: younger age of onset, a long disease duration, lack of PSWCs on EEG, positive CSF biomarkers, prominent MRI cortical ribboning including hippocampal involvement, severe vacuolation in many cortical regions and the striatum, and similar cortical and striatal distributions of PrP^{Sc} deposition. Unlike most sCJD VV1 cases, however, our patient had striatal DWI hyperintensity and diffuse PrP^{Sc} in the cerebellar cortex, including the granular layer [33, 34].

Four unique lines of Tg mice expressing HuPrP(V129,A224V) at levels of up to ~3× failed to develop any signs of spontaneous neurological illness for more than 600 days, failing to support the hypothesis that the A224V mutation is pathological. However, many lines of Tg mice expressing PrP alleles containing familial prion disease-causing mutations do not develop spontaneous disease (reviewed in [35]). In particular, the context of the mutation may

Author Manuscript Author Manuscript Author Manuscript Author Manuscript

play an important role. For example, knock-in mice expressing MoPrP containing the disease-causing E200K mutation develop spontaneous disease [36], as do Tg mice expressing a chimeric mouse/human PrP with the mutation [37]. In contrast, E200K does not cause disease in Tg mice when present in a HuPrP backbone [38]. Similarly, the P102L GSS mutation causes disease in Tg mice when present in a MoPrP [39–41] but not a HuPrP backbone [38]. Thus, the lack of spontaneous disease in Tg(HuPrP,V129,A224V) mice does not necessarily imply that A224V is a benign polymorphism as opposed to a disease-causing mutation or risk factor. We chose a HuPrP(V129) backbone for investigating the effects of the A224V mutation on prion formation and transmission since replication of sCJD VV2 prions in Tg mice expressing chimeric mouse/human PrP with the V129 polymorphism is inefficient [42].

A single amino acid mismatch between PrP^{Sc} in the inoculum and PrP^{C} in the recipient animal is often sufficient to prolong incubation periods in bioassays [43], likely due to the introduction of a transmission barrier. In contrast, we found that inoculation of Tg(HuPrP,V129,A224V) mice with sCJD VV2 prions (which do not contain the A224V mutation) dramatically accelerated disease transmission without altering the strain properties of the sCJD VV2 isolate, arguing for an effect on prion replication kinetics rather than modulating a transmission barrier. The A224V mutation is located within the third α-helix of the C-terminal structured domain of HuPrP [44], proximal to the GPI-anchor attachment site. Prion disease-causing missense mutations, other than those that generate anchorless PrP variants in GSS patients [45], have not previously been reported in this region of PrP. The increased hydrophobicity conferred by the presence of valine at residue 224 may slightly alter the conformation of PrP^{C}, its orientation relative to the cellular membrane, its interaction with membrane lipids or proteins [46], or its affinity for prion replication cofactors [15, 47], all of which may potentially affect the kinetics of prion formation. Alternatively, the mutation may affect the kinetics of prion spreading via axonal or transneuronal transport, which may be important for the propagation of prions in many neurodegenerative diseases [48, 49].

Acknowledgments

We thank the staff at the Hunter's Point animal facility for their assistance with the animal experiments, Marta Gavidia for mouse genotyping, and Dr. Pierluigi Gambetti and the National Prion Disease Pathology Surveillance Center for providing the sCJD VV1 sample and the genetic analysis of the CJD(A224V) case. This work was supported by research grants from the National Institutes of Health (NIH AG021601, AG002132, AG010770) as well as gifts from the Sherman Fairchild Foundation and the Fight for Mike Program. J.C.W. was supported by a K99 grant (AG042453) from the National Institute on Aging (NIA). M.D.G. was supported by an NIH/NIA grant (R01 AG031189).

References

1. Colby DW, Prusiner SB. Prions. Cold Spring Harb Perspect Biol. 2011; 3:a006833. [PubMed: 21421910]
2. McKinley MP, Bolton DC, Prusiner SB. A protease-resistant protein is a structural component of the scrapie prion. Cell. 1983; 35:57–62. [PubMed: 6414721]
3. Parchi P, Giese A, Capellari S, et al. Classification of sporadic Creutzfeldt-Jakob disease based on molecular and phenotypic analysis of 300 subjects. Ann Neurol. 1999; 46:224–233. [PubMed: 10443888]

Author Manuscript Author Manuscript Author Manuscript Author Manuscript

4. Bessen RA, Kocisko DA, Raymond GJ, et al. Non-genetic propagation of strain-specific properties of scrapie prion protein. Nature. 1995; 375:698–700. [PubMed: 7791905]
5. Telling GC, Parchi P, DeArmond SJ, et al. Evidence for the conformation of the pathologic isoform of the prion protein enciphering and propagating prion diversity. Science. 1996; 274:2079–2082. [PubMed: 8953038]
6. Parchi P, Strammiello R, Notari S, et al. Incidence and spectrum of sporadic Creutzfeldt-Jakob disease variants with mixed phenotype and co-occurrence of PrP^{Sc} types: an updated classification. Acta Neuropathol. 2009; 118:659–671. [PubMed: 19718500]
7. Collins SJ, Sanchez-Juan P, Masters CL, et al. Determinants of diagnostic investigation sensitivities across the clinical spectrum of sporadic Creutzfeldt-Jakob disease. Brain. 2006; 129:2278–2287. [PubMed: 16816392]
8. Korth C, Kaneko K, Groth D, et al. Abbreviated incubation times for human prions in mice expressing a chimeric mouse—human prion protein transgene. Proc Natl Acad Sci US A. 2003; 100:4784–4789.
9. Bishop MT, Will RG, Manson JC. Defining sporadic Creutzfeldt-Jakob disease strains and their transmission properties. Proc Natl Acad Sci USA. 2010; 107:12005–12010. [PubMed: 20547859]
10. Berry DB, Lu D, Geva M, et al. Drug resistance confounding prion therapeutics. Proc Natl Acad Sci US A. 2013; 110:E4160–E4169.
11. Büeler H, Fisher M, Lang Y, et al. Normal development and behaviour of mice lacking the neuronal cell-surface PrP protein. Nature. 1992; 356:577–582. [PubMed: 1373228]
12. Watts JC, Giles K, Stöhr J, et al. Spontaneous generation of rapidly transmissible prions in transgenic mice expressing wild-type bank vole prion protein. Proc Natl Acad Sci US A. 2012; 109:3498–3503.
13. Stanker LH, Serban AV, Cleveland E, et al. Conformation-dependent high-affinity monoclonal antibodies to prion proteins. J Immunol. 2010; 185:729–737. [PubMed: 20530267]
14. Safar JG, Scott M, Monaghan J, et al. Measuring prions causing bovine spongiform encephalopathy or chronic wasting disease by immunoassays and transgenic mice. Nat Biotechnol. 2002; 20:1147–1150. [PubMed: 12389035]
15. Telling GC, Scott M, Mastrianni J, et al. Prion propagation in mice expressing human and chimeric PrP transgenes implicates the interaction of cellular PrP with another protein. Cell. 1995; 83:79–90. [PubMed: 7553876]
16. Watts JC, Giles K, Patel S, et al. Evidence that bank vole PrP is a universal acceptor for prions. PLoS Pathog. 2014; 10:e1003990. [PubMed: 24699458]
17. Zerr I, Bodemer M, Räcker S, et al. Cerebrospinal fluid concentration of neuron-specific enolase in diagnosis of Creutzfeldt-Jakob disease. Lancet. 1995; 345:1609–1610. [PubMed: 7783539]
18. Otto M, Wiltfang J, Cepek L, et al. Tau protein and 14-3-3 protein in the differential diagnosis of Creutzfeldt-Jakob disease. Neurology. 2002; 58:192–197. [PubMed: 11805244]
19. Young GS, Geschwind MD, Fischbein NJ, et al. Diffusion-weighted and fluid-attenuated inversion recovery imaging in Creutzfeldt-Jakob disease: high sensitivity and specificity for diagnosis. Am J Neuroradiol. 2005; 26:1551–1562. [PubMed: 15956529]
20. Vitali P, Maccagnano E, Caverzasi E, et al. Diffusion-weighted MRI hyperintensity patterns differentiate CJD from other rapid dementias. Neurology. 2011; 76:1711–1719. [PubMed: 21471469]
21. Westaway D, DeArmond SJ, Cayetano-Canlas J, et al. Degeneration of skeletal muscle, peripheral nerves, and the central nervous system in transgenic mice overexpressing wild-type prion proteins. Cell. 1994; 76:117–129. [PubMed: 8287472]
22. Asante EA, Linehan JM, Desbruslais M, et al. BSE prions propagate as either variant CJD-like or sporadic CJD-like prion strains in transgenic mice expressing human prion protein. EMBO J. 2002; 21:6358–6366. [PubMed: 12456643]
23. Shiga Y, Satoh K, Kitamoto T, et al. Two different clinical phenotypes of Creutzfeldt-Jakob disease with a M232R substitution. J Neurol. 2007; 254:1509–1517. [PubMed: 17965961]
24. Beck JA, Poulter M, Campbell TA, et al. *PRNP* allelic series from 19 years of prion protein gene sequencing at the MRC Prion Unit. Hum. Mutat. 2010; 31:E1551–E1563.
25. Exome Aggregation Consortium (ExAC). Cambridge, MA: 2014. http://exac.broadinstitute.org

Author Manuscript Author Manuscript Author Manuscript Author Manuscript

26. Pocchiari M, Salvatore M, Cutruzzola F, et al. A new point mutation of the prion protein gene in familial and sporadic cases of Creutzfeldt-Jakob disease. Ann Neurol. 1993; 34:802–807. [PubMed: 7902693]
27. Spudich S, Mastrianni JA, Wrensch M, et al. Complete penetrance of Creutzfeldt-Jakob disease in Libyan Jews carrying the E200K mutation in the prion protein gene. Mol Med. 1995; 1:607–613. [PubMed: 8529127]
28. Poduri A, Evrony GD, Cai X, Walsh CA. Somatic mutation, genomic variation, and neurological disease. Science. 2013; 341:1237758. [PubMed: 23828942]
29. Palmer MS, Dryden AJ, Hughes JT, Collinge J. Homozygous prion protein genotype predisposes to sporadic Creutzfeldt-Jakob disease. Nature. 1991; 352:340–342. [PubMed: 1677164]
30. Krasnianski A, Bartl M, Sanchez Juan PJ, et al. Fatal familial insomnia: Clinical features and early identification. Ann Neurol. 2008; 63:658–661. [PubMed: 18360821]
31. Kong, Q.; Surewicz, WK.; Petersen, RB., et al. Inherited prion diseases. In: Prusiner, SB., editor. Prion Biology and Diseases. 2. Cold Spring Harbor: Cold Spring Harbor Laboratory Press; 2004. p. 673-775.
32. Nonno R, Di Bari MA, Cardone F, et al. Efficient transmission and characterization of Creutzfeldt-Jakob disease strains in bank voles. PLoS Pathog. 2006; 2:e12. [PubMed: 16518470]
33. Meissner B, Westner IM, Kallenberg K, et al. Sporadic Creutzfeldt-Jakob disease: clinical and diagnostic characteristics of the rare VV1 type. Neurology. 2005; 65:1544–1550. [PubMed: 16221949]
34. Tanev KS, Yilma M. An unusually presenting case of sCJD--the VV1 subtype. Clin Neurol Neurosurg. 2009; 111:282–291. [PubMed: 18995952]
35. Watts JC, Prusiner SB. Mouse models for studying the formation and propagation of prions. J Biol Chem. 2014; 289:19841–19849. [PubMed: 24860095]
36. Jackson WS, Borkowski AW, Watson NE, et al. Profoundly different prion diseases in knock-in mice carrying single PrP codon substitutions associated with human diseases. Proc Natl Acad Sci USA. 2013; 110:14759–14764. [PubMed: 23959875]
37. Friedman-Levi Y, Meiner Z, Canello T, et al. Fatal prion disease in a mouse model of genetic E200K Creutzfeldt-Jakob disease. PLoS Pathog. 2011; 7:e1002350. [PubMed: 22072968]
38. Asante EA, Gowland I, Grimshaw A, et al. Absence of spontaneous disease and comparative prion susceptibility of transgenic mice expressing mutant human prion proteins. J Gen Virol. 2009; 90:546–558. [PubMed: 19218199]
39. Hsiao KK, Scott M, Foster D, et al. Spontaneous neurodegeneration in transgenic mice with mutant prion protein. Science. 1990; 250:1587–1590. [PubMed: 1980379]
40. Telling GC, Haga T, Torchia M, et al. Interactions between wild-type and mutant prion proteins modulate neurodegeneration in transgenic mice. Genes Dev. 1996; 10:1736–1750. [PubMed: 8698234]
41. Nazor KE, Kuhn F, Seward T, et al. Immunodetection of disease-associated mutant PrP, which accelerates disease in GSS transgenic mice. EMBO J. 2005; 24:2472–2480. [PubMed: 15962001]
42. Giles K, De Nicola GF, Patel S, et al. Identification of I137M and other mutations that modulate incubation periods for two human prion strains. J Virol. 2012; 86:6033–6041. [PubMed: 22438549]
43. Manson JC, Jameison E, Baybutt H, et al. A single amino acid alteration (101L) introduced into murine PrP dramatically alters incubation time of transmissible spongiform encephalopathy. EMBO J. 1999; 18:6855–6864. [PubMed: 10581259]
44. Zahn R, Liu A, Lührs T, et al. NMR solution structure of the human prion protein. Proc Natl Acad Sci US A. 2000; 97:145–150.
45. Jansen C, Parchi P, Capellari S, et al. Prion protein amyloidosis with divergent phenotype associated with two novel nonsense mutations in *PRNP*. Acta Neuropathol. 2010; 119:189–197. [PubMed: 19911184]
46. Taylor DR, Whitehouse IJ, Hooper NM. Glypican-1 mediates both prion protein lipid raft association and disease isoform formation. PLoS Pathog. 2009; 5:e1000666. [PubMed: 19936054]

Author Manuscript Author Manuscript Author Manuscript Author Manuscript

47. Deleault NR, Piro JR, Walsh DJ, et al. Isolation of phosphatidylethanolamine as a solitary cofactor for prion formation in the absence of nucleic acids. Proc Natl Acad Sci USA. 2012; 109:8546–8551. [PubMed: 22586108]

48. Saper CB, Wainer BH, German DC. Axonal and transneuronal transport in the transmission of neurological disease: potential role in system degenerations, including Alzheimer's disease. Neuroscience. 1987; 23:389–398. [PubMed: 2449630]

49. Prusiner SB. Biology and genetics of prions causing neurodegeneration. Annu Rev Genet. 2013; 47:601–623. [PubMed: 24274755]

Author Manuscript Author Manuscript Author Manuscript Author Manuscript

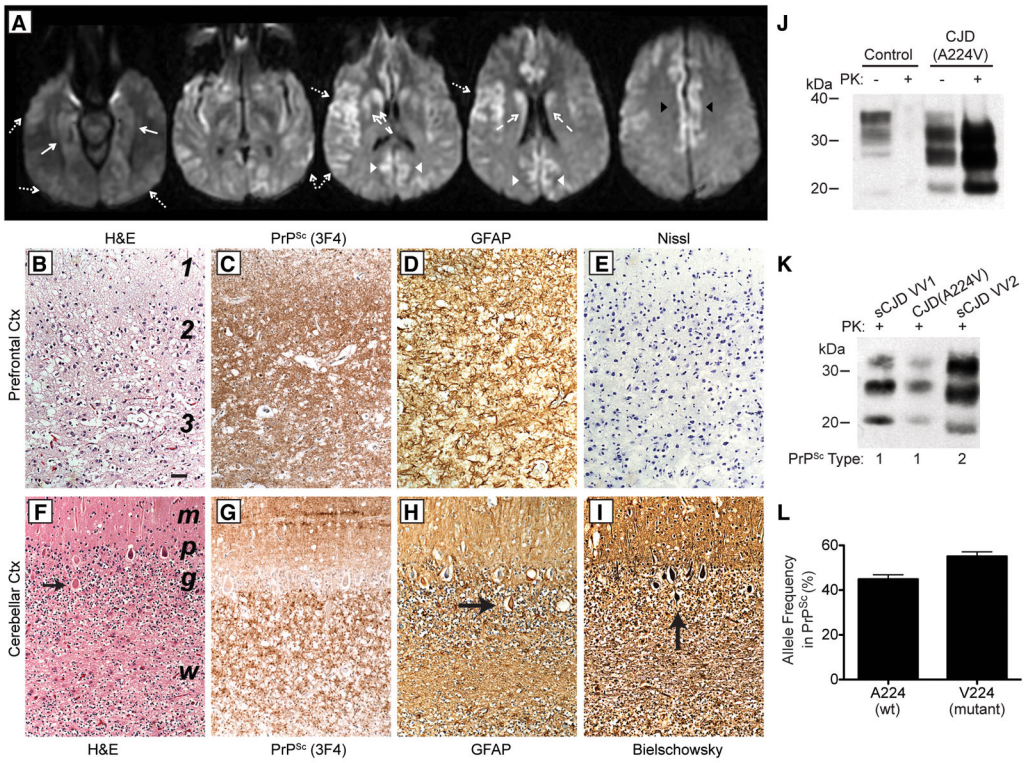

Figure 1. Characterization of the CJD(A224V) patient's brain

(**A**) 1.5T brain MRI with DWI sequences at 10.5 months following disease onset showing hyperintensity with reduced diffusion involving the cortex of the middle and superior frontal gyri, bilateral insula, bilateral hippocampi (solid arrows), bilateral cingulate gyri (black arrowheads), bilateral caudate and anterior putamen (dashed arrows), bilateral occipital (white arrowheads) and temporal cortex (dotted arrows). (**B**–**I**) Neuropathological analysis of the CJD(A224V) patient. Sections of the prefrontal cortex (**B**–**E**) and the cerebellar cortex (**F**–**I**) show features of severe CJD. (**B, F**) H&E stain reveals status spongiosis in cortical layers 1–3 and marked nerve cell loss in layers 2 and 3 (**B**) and spongiform degeneration of the molecular layer, Purkinje nerve cell loss, and at least 50% granule cell neuron loss (**F**). Arrow indicates a torpedo along the proximal portion of a Purkinje cell axon. (**C, G**) Immunostaining with 3F4 reveals dense finely granular staining for PrP^{Sc} with less intense staining in layer 1 (**C**) and abundant PrP^{Sc} deposition in the molecular layer and granule cell layer (**G**). (**D, H**) GFAP immunostaining shows severe reactive astrocytic gliosis in all layers (**D**), and reactive Bergman radial glia in the molecular layer and reactive astrocytes in the granule cell layer and underlying white matter (**H**). Arrow indicates a torpedo. (**E**) The Nissl stain verifies marked nerve cell loss in layers 2 and 3. (**I**) The Bielschowsky silver stain strongly stains a Purkinje cell torpedo (arrow). Bar in B represents 100 μm and applies to all photomicrographs. In B, numbers denote cerebral cortical layers. In F, regions of the cerebellar cortex are indicated: *m*, molecular layer; *p*, Purkinje cell layer; *g*, granule cell layer; *w*, white matter. (**J**) Immunoblot of brain homogenates from a control (non-neurodegenerative disease) patient and the CJD(A224V) patient with (+) or without (−) digestion with PK. (**K**) Immunoblot of PK-resistant PrP^{Sc} in the brain of the CJD(A224V) patient reveals a Type-1 signature (migration to ~21 kDa) similar to that observed in an

Author Manuscript Author Manuscript Author Manuscript Author Manuscript

sCJD VV1 patient. In J and K, PrP was detected using the antibody HuM-P. (**L**) Quantification of the relative amounts of wt (A224) and mutant (V224) PK-resistant PrP^{Sc} in the brain of the CJD(A224V) patient. Approximately equal proportions of wt and mutant PrP^{Sc} were found (no significant difference: $P = 0.08$ by the t-test). Data (mean ± SEM) from 4 technical replicates are shown.

Author Manuscript Author Manuscript Author Manuscript Author Manuscript

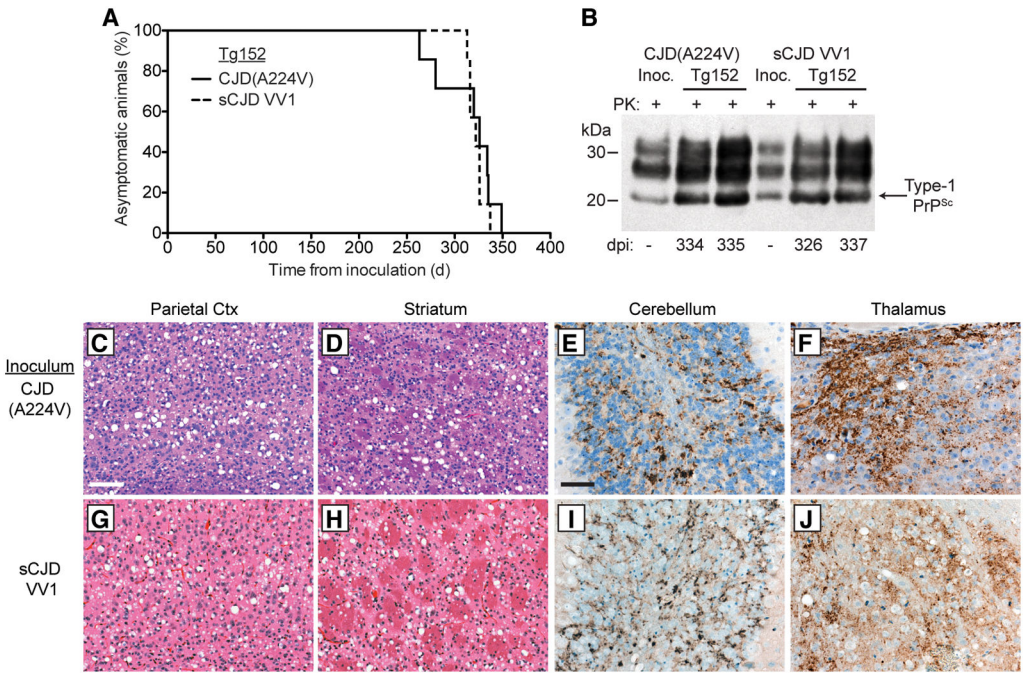

Figure 2. Transmission of CJD(A224V) to transgenic mice

(**A**) Kaplan-Meier survival curves for Tg(HuPrP,V129)152 mice inoculated with brain homogenate from either the CJD(A224V) patient (solid black line, *n* = 7) or an sCJD VV1 patient (dashed black line, *n* = 7). The curves were not significantly different by the Log-rank test (*P* = 0.56). (**B**) Immunoblot of PK-resistant PrP^{Sc} in the brains of clinically ill Tg152 mice at the indicated days postinoculation (dpi) with either CJD(A224V) or sCJD VV1 brain homogenate. PrP^{Sc} profiles in the human brain homogenates used for inoculation ("Inoc.") are shown for comparison. PK-resistant PrP was detected using the antibody HuM-P. (**C**–**J**) Neuropathological characterization of CJD-inoculated Tg152 mice. Brain sections from clinically ill mice at 313–337 dpi with either CJD(A224V) (**C**–**F**) or sCJD VV1 (**G**–**J**) brain homogenate were analyzed by H&E staining (**C**, **D**, **G**, and **H**) or by immunostaining for PrP (**E**, **F**, **I**, and **J**). Prominent spongiform degeneration was observed in the parietal cortex (**C**, **G**) and striatum (**D**, **H**), and abundant granular PrP^{Sc} deposition was observed in the granule cell layer of the cerebellum (**E**, **I**) as well as the thalamus (**F**, **J**). PrP^{Sc} deposits were visualized using the antibody 3F4. Scale bar in C represents 100 μm and also applies to panels D, G, and H; scale bar in E represents 50 μm and also applies to panels F, I, and J.

Author Manuscript Author Manuscript Author Manuscript Author Manuscript

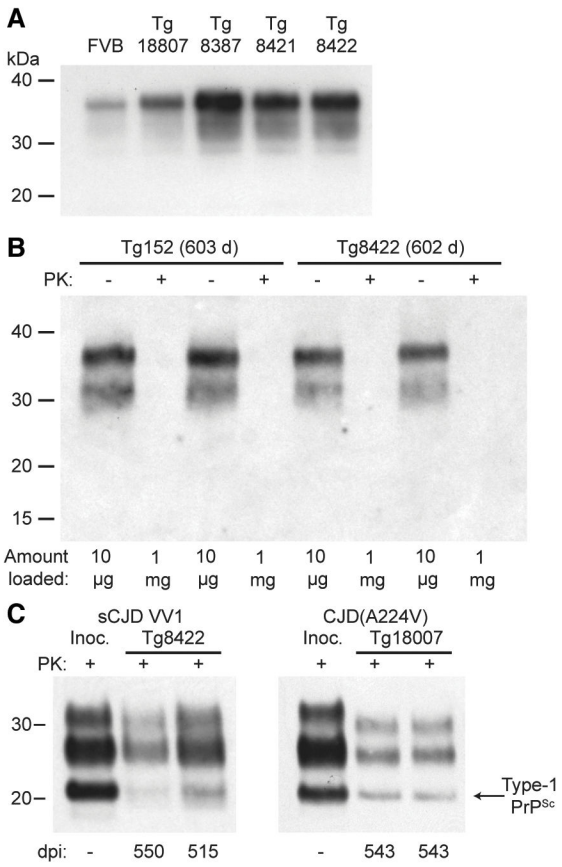

Figure 3. Tg(HuPrP,V129,A224V) mice do not develop spontaneous disease

(**A**) Immunoblot of PrP in undigested brain homogenates from wt FVB mice and four distinct lines of Tg(HuPrP,V129,A224V) mice. (**B**) Immunoblot of total PrP in undigested (−) brain homogenates or insoluble PrP following PK digestion (+) of brain homogenates from aged Tg(HuPrP,V129)152 and Tg(HuPrP,V129,A224V)8422 mice. Note that 100 times more material was loaded for the PK-digested samples. (**C**) Immunoblot of PK-resistant PrP^{Sc} in the brains of clinically ill Tg8422 mice at the indicated dpi with sCJD VV1 prions (left) or asymptomatic Tg18807 mice at the indicated days postinoculation (dpi) with CJD(A224V) prions (right). The PrP^{Sc} profiles in the human brain homogenates used for inoculation (“Inoc.”) are shown for comparison. In all panels, PrP was detected using the antibody HuM-P.

Author Manuscript Author Manuscript Author Manuscript Author Manuscript

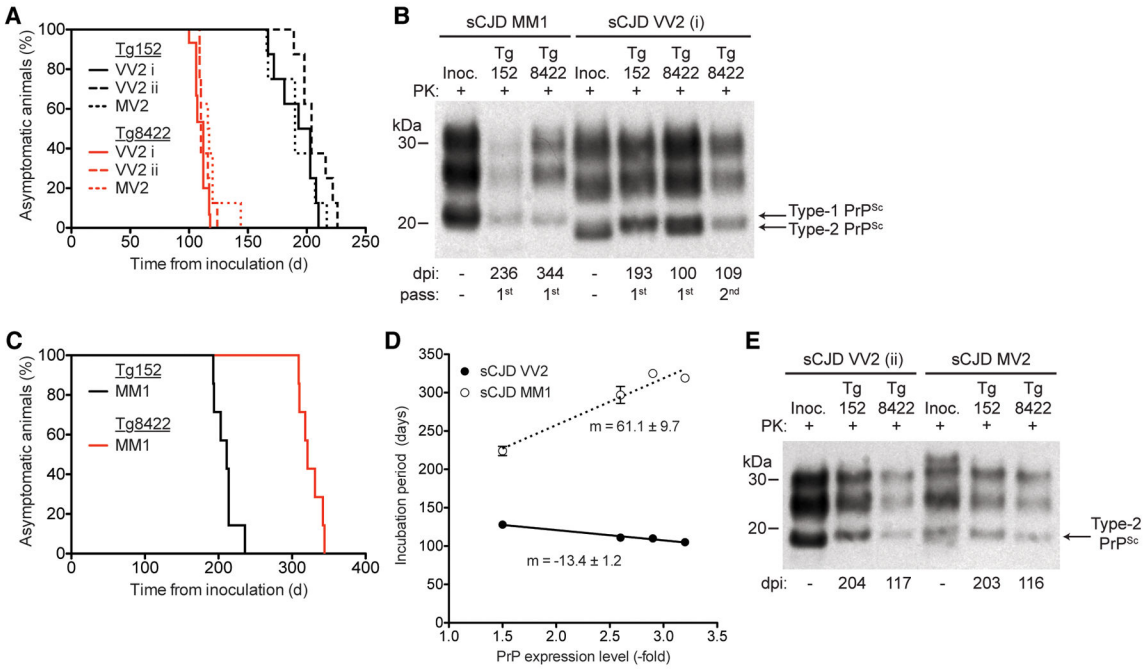

Figure 4. Accelerated transmission of sCJD VV2 and MV2 prions to Tg(HuPrP,V129,A224)8422 mice

(**A**) Kaplan-Meier survival curves for Tg152 mice (black lines) and Tg8422 mice (red lines) inoculated with sCJD VV2 case i (solid lines, *n* = 8 and 15, respectively), sCJD VV2 case ii (dashed lines, *n* = 8 each), or sCJD MV2 (dotted lines, *n* = 8 each) prions. The presence of the A224V mutation significantly accelerated the onset of neurologic illness in VV2- and MV2-inoculated mice ($P < 0.001$ by the Log-rank test). (**B**) Immunoblot of PK-resistant PrP^{Sc} in the brains of clinically ill Tg152 or Tg8422 mice injected with sCJD MM1 or sCJD VV2 (case i) prions (1^{st} or 2^{nd} passage) at the indicated days postinoculation (dpi). (**C**) Kaplan-Meier survival curves for Tg152 mice (black line, *n* = 7) and Tg8422 mice (red line; *n* = 7) inoculated with brain homogenate from an sCJD MM1 patient. The presence of the A224V mutation significantly delayed the onset of neurologic illness in MM1-inoculated mice ($P < 0.001$ by the Log-rank test). (**D**) Correlation of PrP expression levels and incubation periods following inoculation of Tg(HuPrP,V129,A224V) mice with sCJD MM1 prions (dotted line) or VV2 case i prions (solid line). As determined by linear regression, there was a direct relationship (positive slope) between PrP expression level and incubation period in MM1-inoculated mice and an inverse relationship (negative slope) in VV2-inoculated mice. (**E**) Immunoblot of PK-resistant PrP^{Sc} in the brains of clinically ill Tg152 or Tg8422 mice injected with sCJD VV2 (case ii) or sCJD MV2 prions at the indicated dpi. PrP^{Sc} profiles in the human brain homogenates used for inoculation ("Inoc.") are shown for comparison. In panels B and E, PK-resistant PrP was detected using the antibody HuMP.

Author Manuscript Author Manuscript Author Manuscript Author Manuscript

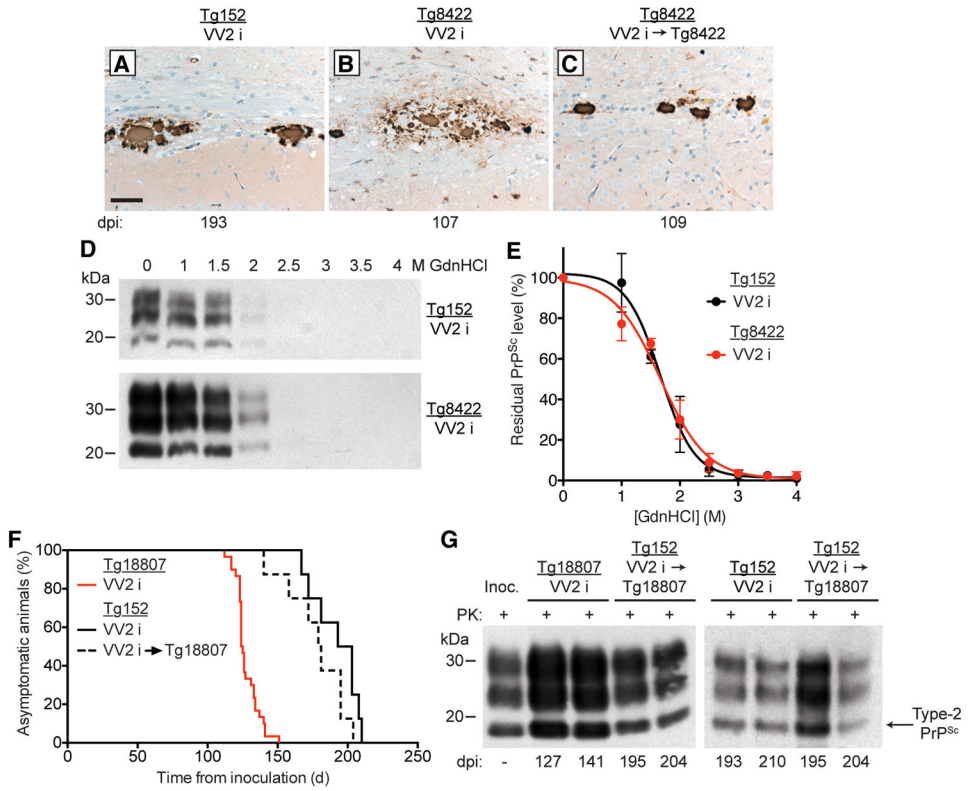

Figure 5. Passage of sCJD VV2 case i prions in Tg(HuPrP,V129,A224V) mice did not alter the prion strain properties

(**A**–**C**) Immunohistochemical detection of PrP^{Sc} deposition in the brains of sCJD VV2-inoculated Tg mice at the indicated days postinoculation (dpi). Plaque-like PrP^{Sc} deposits in the corpus callosum were observed in Tg152 mice (**A**) and Tg8422 mice (**B**, **C**) following one (**A**, **B**) or two (**C**) passages of sCJD VV2 prions. PrP^{Sc} deposits were detected using the antibody 3F4. Scale bar in A represents 50 μm and also applies to panels B and C. (**D**) Representative immunoblots and (**E**) denaturation curves (n = 3 brains per group) of residual PK-resistant PrP^{Sc} levels after conformational stability assays in brain homogenates from clinically ill Tg152 and Tg8422 mice inoculated with sCJD VV2 prions. No significant difference in the $[GdnHCl]_{1/2}$ values was observed for sCJD VV2 prions upon propagation in Tg152 or Tg8422 mice (P = 0.57 by the Extra sum-of-squares F-test). (**F**) Kaplan-Meier survival curves for sCJD VV2-inoculated Tg152 (solid black line; n = 8) or Tg18807 (red line; n = 30) mice as well as Tg152 mice inoculated with sCJD VV2 prions that had been passaged once in Tg18807 mice (dashed black line; n = 8). There was no significant difference in the survival curves for the two groups of inoculated Tg152 mice (P = 0.15 by the Log-rank test). (**G**) Immunoblots of PK-resistant PrP^{Sc} in the brains of clinically ill Tg152 or Tg18807 mice infected with sCJD VV2 prions as well as Tg152 mice inoculated with sCJD VV2 prions passaged once in Tg18807 mice. The incubation period for each mouse is indicated as days postinoculation (dpi). The PrP^{Sc} profile in the sCJD VV2 human brain homogenate used for the original inoculation (“Inoc.”) is shown for comparison. In panels D and G, PrP was detected using the antibody HuM-P.

Author Manuscript Author Manuscript Author Manuscript Author Manuscript

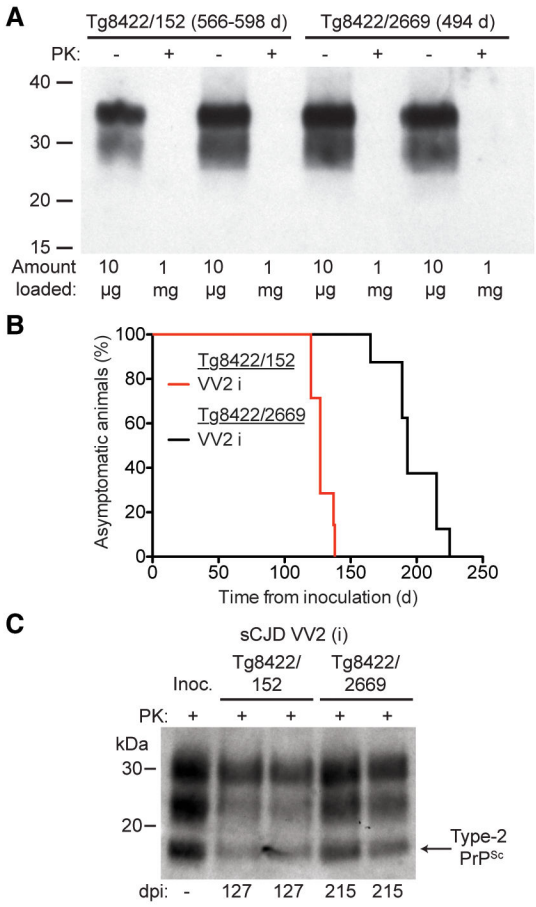

Figure 6. Replication of sCJD VV2 prions in bigenic mice coexpressing wt and mutant A224V HuPrP alleles

(**A**) Immunoblot of total PrP in undigested (−) brain homogenates or insoluble PrP following PK digestion (+) of brain homogenates from aged Tg8422/152 mice coexpressing mutant HuPrP(V129,A224V) and wt HuPrP(V129) and Tg8422/2669 mice coexpressing mutant HuPrP(V129,A224V) and wt HuPrP(M129). Note that 100 times more material was loaded for the PK-digested samples. (**B**) Kaplan-Meier survival curves for Tg8422/152 mice (red line; $n = 7$) and Tg8422/2669 mice (black line; $n = 8$) following inoculation with sCJD VV2 case i prions. The presence of wt HuPrP(M129) in *trans* significantly delayed the onset of neurologic illness in VV2-inoculated mice ($P < 0.001$ by the Log-rank test). (**C**) Immunoblot of PK-resistant PrP^{Sc} in the brains of clinically ill, sCJD VV2-inoculated Tg8422/152 and Tg8422/2669 mice at the indicated days postinoculation (dpi). PK-resistant PrP^{Sc} in the sCJD VV2 inoculum ("Inoc.") is shown for comparison. In panels A and C, PrP was detected using the antibody HuM-P.

Author Manuscript Author Manuscript Author Manuscript Author Manuscript

Table 1

Influence of the A224V mutation on the incubation periods for CJD VV1, MM1, and VV2 prions in transgenic mice

Mouse line	PrP Expression Level (-fold)*	Mean incubation period ± SEM, in days (n/n_0)¶						
		Uninoculated	CJD(A224V)	sCJD VV1	sCJD VV2 (i)	sCJD VV2 (i)2nd passage	sCJD MM1	sCJD MM12nd passage
Tg(HuPrP,V129)19273	2.6	> 603 (0/7)	—	—	208 ± 5 (7/7)	—	206 ± 3 (7/7)	—
Tg(HuPrP,V129)152	3.4	> 603 (0/7)	315 ± 12 (7/7)	322 ± 3 (7/7)	192 ± 6 (8/8)	—	209 ± 6 (7/7)	—
Tg(HuPrP,V129)7879	4.3	> 604 (0/6)	—	—	222 ± 4 (7/7)	—	222 ± 3 (8/8)	—
Tg(HuPrP,V129)19272	4.5	> 602 (0/6)	336 ± 14 (7/7)	—	215 ± 4 (7/7)	—	233 ± 3 (8/8)	—
Tg(HuPrP,V129,A224V)18807	1.5	> 600 (0/19)	> 533 (0/7)	—	128 ± 2 (30/30)	126 ± 4 (6/6)	224 ± 6 (8/8)	252 ± 11 (6/6)
Tg(HuPrP,V129,A224V)8421	2.6	> 600 (0/7)	—	—	111 ± 1 (6/6)	—	297 ± 11 (8/8)	—
Tg(HuPrP,V129,A224V)8422	2.9	> 602 (0/7)	> 503 (0/7)§	541 ± 9 (4/7)	110 ± 1 (15/15)	112 ± 4 (7/7)	325 ± 5 (7/7)	—
Tg(HuPrP,V129,A224V)8387	3.2	> 601 (0/7)	—	—	105 ± 4 (7/7)	—	319 ± 5 (7/7)	—

n, number of mice with clinical signs of neurologic dysfunction; n_0, number of examined mice.

*compared to PrP expression in wild-type mice.

¶For uninoculated mice, incubation periods represent the age of the mice; for all other experiments, incubation periods represent days postinoculation.

§One mouse exhibited bradykinesia, blank stare, and circling behavior at 386 dpi but was negative for PK-resistant PrP^{Sc} and prion disease-specific neuropathology.

Author Manuscript Author Manuscript Author Manuscript Author Manuscript

Table 2

Coexpression of mutant and wild-type human PrP transgenes in bigenic mice inoculated with sCJD VV2 prions.

Mouse line	Mean incubation period ± SEM, in days (n/n_0)¶			
	Uninoculated	sCJD VV2 (i)	sCJD VV2 (ii)	sCJD MV2
Tg(HuPrP,V129)152	> 603 (0/7)	192 ± 6 (8/8)	207 ± 5 (8/8)	191 ± 6 (8/8)
Tg(HuPrP,V129,A224V)8422	> 602 (0/7)	110 ± 1 (15/15)	113 ± 2 (8/8)	118 ± 4 (8/8)
Tg(HuPrP,V129,A224V)8422 × Tg(HuPrP,V129)152	566 ± 0 (3/6)	128 ± 3 (7/7)	—	—
Tg(HuPrP,V129,A224V)8422 × Tg(HuPrP,M129)2669	490 ± 11 (8/12)	198 ± 7 (8/8)	—	—

n, number of mice with clinical signs of neurologic dysfunction; n_0, number of examined mice.

¶For uninoculated mice, incubation periods represent the age of the mice; for all other experiments, incubation periods represent days postinoculation.

Ann Neurol. Author manuscript; available in PMC 2016 October 01.